

Using the Transport of Intensity and the Transport of Phase Equation for Phase Retrieval

Clemens Kirisits¹
clemens.kirisits@univie.ac.at

Kemal Raik¹
kemal.raik@univie.ac.at

Otmar Scherzer^{1,2,3}
otmar.scherzer@univie.ac.at

Christina Strohmenger¹
christina.ulrike.strohmenger@univie.ac.at

Jikai Yan¹
jikai.yan@univie.ac.at

¹Faculty of Mathematics
University of Vienna
Oskar-Morgenstern-Platz 1
A-1090 Vienna, Austria

²Johann Radon Institute for Computational
and Applied Mathematics (RICAM)
Altenbergerstraße 69
A-4040 Linz, Austria

³Christian Doppler Laboratory
for Mathematical Modeling and Simulation
of Next Generations of Ultrasound Devices (MaMSi)
Oskar-Morgenstern-Platz 1
A-1090 Vienna, Austria

Abstract

We investigate the transport of intensity equation (TIE) and the transport of phase equation (TPE) for solving the phase retrieval problem. Both the TIE and the TPE are derived from the paraxial Helmholtz equation and relate phase information to the intensity. The TIE is usually favored since the TPE is nonlinear. The main contribution of this paper is that we discuss situations in which it is possible to use the two equations in a hybrid manner: We show that 2-dimensional phase information retrieved by the TIE can be used as initial data for the TPE, enabling the acquisition of 3-dimensional phase information. The latter is solved using the method of characteristic and viscosity methods. Both the TIE and the viscosity method are numerically implemented with finite element methods.

1. INTRODUCTION

The phase retrieval problem consists in computing the phase $\phi : \mathbb{R}^3 \rightarrow \mathbb{R}$ of a complex valued function

$$\begin{aligned} A : \mathbb{R}^3 &\rightarrow \mathbb{C}, \\ (\mathbf{x}, z) &\mapsto \sqrt{I(\mathbf{x}, z)} \exp(i\phi(\mathbf{x}, z)) \end{aligned} \quad (1.1)$$

given measurements of the intensity I . Since typically the phase is harder to measure than the intensity but the phase describes the specimen more appropriately, the phase retrieval problem has several applications in the fields of microscopy [19], holography and crystallography (see for instance [9]). There exist experimental setups, such as interferometers [8, 4, 9] and computational algorithms for phase retrieval, examples for the latter being the Gerchberg-Saxton algorithm [10] and the Hybrid Input-Out method proposed by Fienup [7].

One approach for solving the phase retrieval problem in the case that the illuminating wave is traveling preferential in the z -direction consists in solving the **Transport of Intensity Equation** (TIE)

$$\nabla_{\mathbf{x}} \cdot [I(\mathbf{x}, z) \nabla_{\mathbf{x}} \phi(\mathbf{x}, z)] = k I_z(\mathbf{x}, z) \quad (1.2)$$

for the phase ϕ . The equation was originally proposed by Teague [18] and has been successfully applied in microscopy to reconstruct the phase ϕ from intensity measurements I (see [2]). Several numerical methods to solve this equation have been studied in the literature: In [18] an auxiliary function $\nabla_{\mathbf{x}} \psi = I \nabla_{\mathbf{x}} \phi$ is used to convert the problem into finding the solution of a Poisson equation

$$\nabla_{\mathbf{x}}^2 \psi = k I_z(\mathbf{x}, z). \quad (1.3)$$

The solution can then be plugged into a second Poisson equation, $\nabla_{\mathbf{x}}^2 \phi = \nabla_{\mathbf{x}} \cdot [\frac{1}{I} \nabla_{\mathbf{x}} \psi]$, which may then be solved with a Green's function. The implementation is based on FFT methods to compute the inverse

of the Laplacian operator. FFT methods inherently assume periodic boundary conditions. [12] solve the TIE under Neumann boundary conditions making use of a Zernike polynomial decomposition. Bostan et al [2] use regularisation methods to find the solution of the TIE under periodic boundary conditions. They also rewrite the TIE as a Poisson equation by assuming that the intensity is constant. By measuring the intensity along the transverse direction, the TIE is solved. As we show below, boundary conditions are important to determine the correct phase (see Section 3.1 and Section 3.2). One alternative approach, which avoids specification of boundary conditions is by considering the TIE in free space with a solution in a Sobolev space. The difficulty associated with this strategy is that I has compact support, such that ellipticity of the differential operator in Equation 1.2 is violated, and moreover, Green's kernel needs to be computed for general I , which is difficult. See [5], for the analysis of the decay rate of the solution of the integral equation with the associated Green function as kernel, which formally implies zero boundaries at infinity. We emphasize that Equation 1.3 of [18] is an attempt to avoid using the Green function with diffusion coefficient I .

The starting point for this paper is the following interesting observation: In Section 2 we derive the TIE from the Helmholtz equation assuming that the wave travels mainly in the z -direction. We will see that when deriving the TIE, a second equation, the **Transport of Phase Equation** (TPE)

$$2k\phi_z(\mathbf{x}, z) - \|\nabla_{\mathbf{x}}\phi(\mathbf{x}, z)\|^2 = -\frac{1}{\sqrt{I(\mathbf{x}, z)}}\Delta_{\mathbf{x}}\left(\sqrt{I(\mathbf{x}, z)}\right) =: -\hat{I}(\mathbf{x}, z) \quad (1.4)$$

appears simultaneously.

Both the TIE and the TPE relate the phase to the intensity of the wave. In this paper we will discuss the question of whether the solutions differ if we use one or the other equation for the reconstruction. Furthermore, in applications such as probes being analyzed under the microscope, the domain of interest is bounded. Therefore, both equations require appropriate boundary data in order to be uniquely solvable. In addition to the above mentioned settings, in [14] homogeneous Dirichlet boundary conditions are used for the reconstructions. [15] considers the TIE with Neumann boundary conditions.

In the following, we give an overview on the information that is required in order to reconstruct the phase based on the TIE and the TPE, respectively. For the simplicity of presentation we consider the equations on the three dimensional cube

$$\Omega = [0, 1]^3 \text{ and } \Omega_z = [0, 1]^2 \times \{z\}.$$

Lastly, we write $\Gamma_z := \partial\Omega_z$ for the boundary of the two-dimensional square Ω_z .

We distinguish between two reconstruction situations, which are illustrated in Figure 1:

Case 1 If measurements of $\phi(\mathbf{x}, z)$ are provided on the boundary Γ_{z^*} , then ϕ can be reconstructed in Ω_{z^*} with the TIE. Additionally, if phase information is available on Γ_z for every $z \in [0, 1]$, then we can reconstruct ϕ on the whole domain Ω .

Case 2 Measurements of $\phi(\mathbf{x}, 0)$, and $\phi_z(\mathbf{x}, 0)$ on Ω_0 are used to reconstruct $\phi(\mathbf{x}, z) \in \Omega$ by solving the TPE. In particular, from measurements of ϕ on Γ_0 and Γ_{z^*} , where $z^* \in [0, 1]$, which is close to 0, we can approximately compute $\phi(\mathbf{x}, 0)$ and $\phi_z(\mathbf{x}, 0)$ on Ω_0 . Using these data we can compute ϕ on Ω with the TPE.

The hybrid constellation of the TIE and the TPE has the advantage that only measurement data of the phase on eight line segments (see Section 4.1 for details) are required to compute ϕ on Ω . On the other hand, the TIE would require boundary data on each boundary Γ_z , $z \in [0, 1]$ as pointed out in Case 1. The disadvantage of Case 2 is that one needs to numerically differentiate measurements of the phase.

However, if the TPE is solved by means of the viscosity method (see Section 4.2), we need boundary data on Γ_z for $z \in [0, 1]$, which requires the same amount of boundary data as the pure TIE approach. In comparison with the method of characteristics the advantage of the viscosity method is that solutions exists in the whole domain Ω .

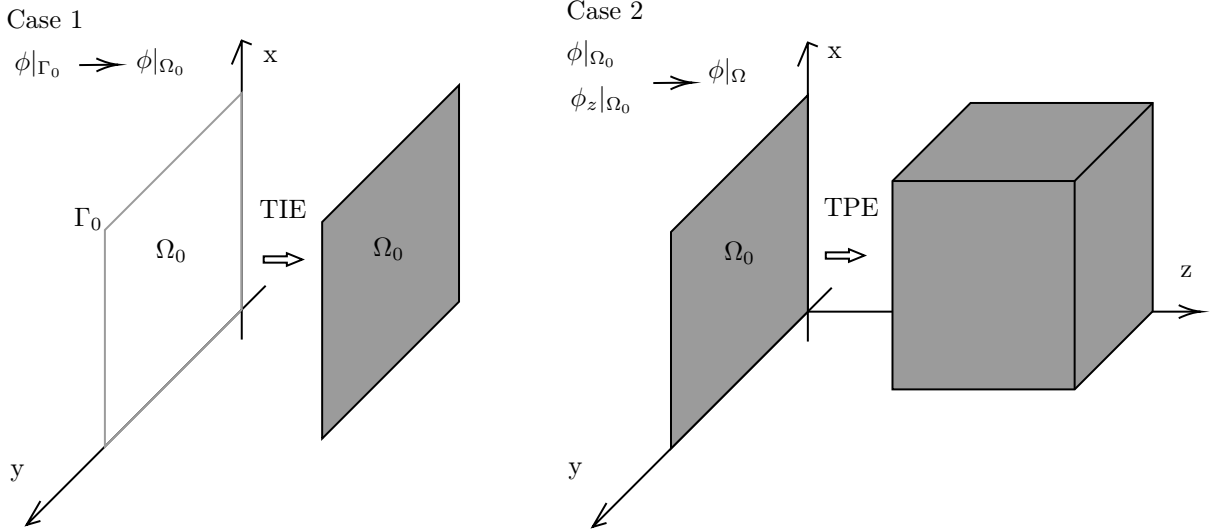


FIGURE 1. Two boundary cases for the TIE and the TPE

The outline of the paper is as follows: In the upcoming section, we will outline the derivation of the TIE and the TPE. Section 3 will be dedicated to solving the TIE numerically for two different phase functions ϕ . Following that, in Section 4, we will thoroughly discuss the TPE, utilizing both the characteristic method and the viscosity method. Finally, in Section 5 we consolidate our findings and discuss the results from Section 3 and Section 4. The TPE is nonlinear. We prove local existence of the solution of the TPE with the method of characteristics (see Section 4.1) and we study viscosity solutions (see [3]) of the TPE in Section 4.2. All presented numerical simulations were implemented with MATLAB.

Notation. For a space-time dependent function $f : \mathbb{R}^3 \times [0, \infty)$, $(x, y, z, t) \mapsto f(x, y, z, t)$ we denote

- the partial derivatives with f_x, f_y, f_z, f_t .
- $\nabla f = (f_x, f_y, f_z)^T$ denotes the spatial gradient of f .
- The n -th partial derivatives are denoted by $f_{\rho_1, \dots, \rho_n}$, where $\rho_i \in \{x, y, z, t\}$.
- $\Delta f = f_{xx} + f_{yy} + f_{zz}$ denotes the three-dimensional Laplace operator in space.
- $\mathbf{x} = (x, y)$ denotes a vector in the xy -plane of the xyz -space \mathbb{R}^3 .
- $\nabla_{\mathbf{x}} f = (f_x, f_y)^T$ denotes the gradient of f with respect to the \mathbf{x} -plane.
- The Laplace operator in the \mathbf{x} -plane is denoted by $\Delta_{\mathbf{x}} = f_{xx} + f_{yy}$.

2. DERIVATION OF THE TRANSPORT OF INTENSITY AND PHASE EQUATIONS

In this section we carry out the derivation of the transport of intensity (TIE) and the transport of phase equation (TPE). For this purpose we derive the paraxial Helmholtz equation first, where we closely follow [12], the details are taken from [11] and [16].

2.1. Paraxial Helmholtz equation. We derive the mathematical equation for a wave u traveling preferably in z direction, the so-called paraxial Helmholtz equation. The starting point is the *scalar wave equation*

$$\frac{n^2}{c^2} u_{tt}(\mathbf{x}, z, t) - \Delta u(\mathbf{x}, z, t) = 0, \quad (2.1)$$

where n represents the refractive index of the medium and c denotes the vacuum velocity of light.

A monochromatic wave with angular velocity ω_0 is given by¹

$$u(\mathbf{x}, z, t) = u_0(\mathbf{x}, z)e^{i\omega_0 t}. \quad (2.2)$$

If u_0 solves the Helmholtz equation

$$\Delta u_0(\mathbf{x}, z) + k^2 u_0(\mathbf{x}, z) = 0 \quad (2.3)$$

with wave number $k := \frac{n\omega_0}{c}$, then the monochromatic wave u solves [Equation 2.1](#).

We follow [\[16\]](#) to derive the *paraxial Helmholtz equation* by making the ansatz

$$u_0(\mathbf{x}, z) = A(\mathbf{x}, z)e^{-ikz} \quad (2.4)$$

and construct A in such a way that u_0 solves [Equation 2.3](#), which means that

$$\begin{aligned} 0 &= \Delta_{\mathbf{x}} (A(\mathbf{x}, z)e^{-ikz}) + \frac{\partial^2}{\partial z^2} (A(\mathbf{x}, z)e^{-ikz}) + k^2 A(\mathbf{x}, z)e^{-ikz} \\ &= e^{-ikz} (\Delta_{\mathbf{x}} A + A_{zz} - 2ikA_z - k^2 A(\mathbf{x}, z)) + k^2 A(\mathbf{x}, z)e^{-ikz}. \end{aligned}$$

After division by the factor e^{-ikz} , we see that A is a solution of

$$\Delta_{\mathbf{x}} A + A_{zz} - 2ikA_z = 0. \quad (2.5)$$

Next, we assume that relative variations of A at scale distance λ are small in comparison with the wavelength $k = \frac{2\pi}{\lambda}$, which means that

$$\frac{|A_z(\mathbf{x}, z)|}{|A(\mathbf{x}, z)|} \sim \frac{1}{\lambda} \frac{|A(\mathbf{x}, z + \lambda) - A(\mathbf{x}, z)|}{|A(\mathbf{x}, z)|} \ll k. \quad (2.6)$$

Note that all dependencies of A are complex. We make the same assumption for A_z , that is

$$\frac{|A_{zz}(\mathbf{x}, z)|}{|A_z(\mathbf{x}, z)|} \ll k, \quad (2.7)$$

and then from [Equation 2.7](#) and [Equation 2.6](#) we deduce that

$$\Delta_{\mathbf{x}} A - 2ikA_z = 0, \quad (2.8)$$

which is the *paraxial Helmholtz equation*.

2.2. Derivation of the TIE and the TPE from the paraxial Helmholtz equation. We use the representation of a complex wave A as in [Equation 1.1](#).

With this representation it follows that,

$$2ikA_z = ke^{i\phi} \left(-2\sqrt{I}\phi_z + i\frac{I_z}{\sqrt{I}} \right)$$

and

$$\Delta_{\mathbf{x}} A = e^{i\phi} \left(-\frac{\|\nabla_{\mathbf{x}} I\|^2}{4I^{\frac{3}{2}}} + \frac{\Delta_{\mathbf{x}} I}{2\sqrt{I}} - \sqrt{I}\|\nabla_{\mathbf{x}} \phi\|^2 + i\sqrt{I}\Delta_{\mathbf{x}} \phi + i\frac{\nabla_{\mathbf{x}} I \cdot \nabla_{\mathbf{x}} \phi}{\sqrt{I}} \right), \quad (2.9)$$

where we left out the spatial variables (\mathbf{x}, z) for notational convenience. Inserting these expressions into the paraxial Helmholtz [Equation 2.8](#) and dividing by $e^{i\phi}$, we get two equations for the real and imaginary part. For the equation resulting from the imaginary part we obtain by multiplication with \sqrt{I} the TIE (see [Equation 1.2](#)). Dividing the real part of equation [Equation 2.9](#) by \sqrt{I} we get the TPE (see [Equation 1.4](#)).

¹The wave function u actually is real-valued and should read as follows $u(\mathbf{x}, z, t) = \Re(u_0(\mathbf{x}, z)e^{i\omega_0 t}) = u_0(\mathbf{x}, z) \cos(\omega t)$. However, it is mathematically convenient to consider the complex extension [Equation 2.2](#).

2.3. Modelling errors of the TIE and the TPE. Both the TIE and the TPE relate the intensity I to the phase ϕ . Therefore, the question arises, whether one of these equations is more accurate, in the sense that the left out second order term in the paraxial approximation affects one of the terms (imaginary part or real part) less than the other. When calculating the second derivative A_{zz} , we obtain

$$A_{zz} = e^{i\phi} \underbrace{\left(-\frac{1}{4} \frac{I_z^2}{I^{\frac{3}{2}}} + \frac{1}{2} \frac{I_{zz}}{\sqrt{I}} - \sqrt{I} \phi_z^2 \right)}_{=:M_{TPE}} + i e^{i\phi} \underbrace{\left(\frac{I_z}{\sqrt{I}} \phi_z + \sqrt{I} \phi_{zz} \right)}_{=:M_{TIE}}.$$

The real and imaginary parts that are omitted describe the modeling errors of the TPE and the TIE, respectively. We see that for the TIE first and second order derivatives of the phase are lost in contrary to the TPE, where only the first order term is lost. However, if one assumes for instance constant intensity of I in the z -direction then the first order term in the TIE loss vanishes, whereas the corresponding lost term for the TPE is still present. In summary, there is no immediate sign that either one of the two equations TIE or TPE is more accurate. Since the TIE is linear for given I and the TPE is nonlinear there is a preference for the TIE, which is why it is used in the literature often [2, 14].

3. THE TRANSPORT OF INTENSITY EQUATION (TIE)

The TIE and the TPE, in Equation 1.2 and Equation 1.4, respectively, where derived in free space \mathbb{R}^3 . For practical computations, however, boundary information on the phase is mandatory and without educated guesses or measurements on the phase at the boundary, the recovered phase information inside Ω cannot be accurate.

In what follows we always assume that the basic assumptions of the theory of elliptic partial differential equations are satisfied (see [13]). In particular, this means that the intensity I of the wave is always positive and the domain is regular. In [1] different types of regularity are discussed, for a detailed discussion of the matter in the context of proving existence and uniqueness results of weak solutions of the TIE we refer to [17].

In the following, we will solve the TIE on $\Omega_0 \subseteq \mathbb{R}^2$ given some Dirichlet boundary condition g on Γ_0 . This corresponds to the first case of the possible settings introduced in Section 1. We will consider the problem

$$\nabla_{\mathbf{x}} \cdot (I \nabla_{\mathbf{x}} \phi) = k I_z \quad \text{in } \Omega_0 \quad \text{and} \quad \phi|_{\Gamma_0} = g,$$

for two different ground-truth functions $A = \sqrt{I} e^{i\phi}$ solving the paraxial Helmholtz equation and we analyze the performance of the TIE for reconstructing the phase ϕ given I .

3.1. Numerical example: constant intensity ($I \equiv 1$). Let $\boldsymbol{\xi} \in \mathbb{R}^2$ be fixed. Then, a short calculation shows that the function

$$A(\mathbf{x}, z) = e^{i(\mathbf{x} \cdot \boldsymbol{\xi} + \frac{1}{2} \|\boldsymbol{\xi}\|^2 z)} \quad \text{for } \mathbf{x} \in \mathbb{R}^2, z \in \mathbb{R}$$

is a solution of the paraxial Helmholtz Equation 2.8 with wavenumber $k = 1$ (see [6]). Comparing with the general form of A in Equation 1.1 we see that

$$I(\mathbf{x}, z) = 1 \quad \text{and} \quad \phi(\mathbf{x}, z) = \mathbf{x} \cdot \boldsymbol{\xi} + \frac{1}{2} \|\boldsymbol{\xi}\|^2 z. \quad (3.1)$$

Figure 2a depicts the function $\mathbf{x} \in \mathbb{R}^2 \rightarrow \phi(\mathbf{x}, 0)$ with $\boldsymbol{\xi} = (1, 1)^T$ as specified in Equation 3.1.

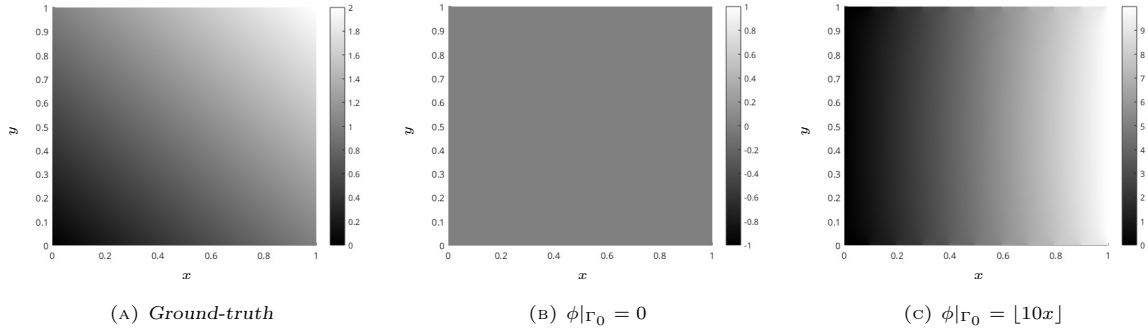


FIGURE 2. Ground-truth of the phase $\phi(\mathbf{x}, z = 0)$ described in Equation 3.1, (left), reconstruction with $\phi|_{\Gamma_0} = 0$ (middle) and $\phi|_{\Gamma_0} = [10x]$ (right)

Since in this case the intensity is constant, the TIE Equation 1.2 reduces to the Laplace equation for ϕ , which we solved for different boundary conditions. The boundary data dominates the outcome and in general we will not be able to retrieve the phase, if we do not impose the ground-truth boundary data given by Equation 3.1 as input data for the reconstruction. The corresponding results for $\phi|_{\Gamma_0} = 0$ and $\phi|_{\Gamma_0} = [10x]$ are depicted in Figure 2b and Figure 2c, respectively. Moreover, the reconstruction of the phase in the $z = 0$ -plane with the ground-truth boundary values is shown in Figure 3a. In addition we also plot the error that is made in the reconstruction (see Figure 3b).

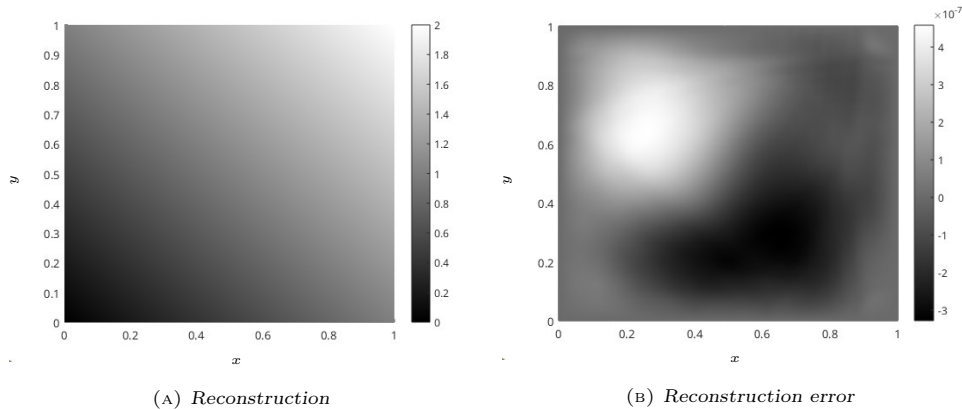


FIGURE 3. Reconstruction (left) and reconstruction error (right) of the phase $\phi(\mathbf{x}, z = 0)$ described in Equation 3.1 given the ground-truth boundary condition

3.2. Numerical example: Constant phase $\phi \equiv \frac{3\pi}{2}$. We have seen that in the case that the intensity is constant but the phase is not, we can reconstruct the phase reasonably well if we impose the boundary condition of the ground-truth on the TIE. Now we consider a numerical example where the phase in the $z = 0$ -plane is constant, whereas the intensity is not. The Gaussian beam (see [16]) is defined by

$$A(\mathbf{x}, z) = I_0 \frac{1}{q(z)} e^{-ik \frac{\|\mathbf{x}\|^2}{2q(z)}}, \quad (3.2)$$

where

$$q(z) := z + iz_R$$

and z_R denotes the so-called Rayleigh range. It serves as an ideal example for testing the reconstruction of the phase by both the TIE and the TPE, since it fulfills the paraxial Helmholtz equation as shown in [16]. We define further

$$w(z) := w_0 \sqrt{1 + \left(\frac{z}{z_R}\right)^2},$$

where w_0 is the waist radius of the Gaussian beam, see [16] for a detailed description.

Furthermore, it holds that

$$\frac{1}{q(z)} = \frac{1}{R(z)} - i \frac{\lambda}{\pi w^2(z)} \quad \text{with } R(z) := z \left(1 + \left(\frac{z_R}{z} \right)^2 \right),$$

such that we can rewrite Equation 3.2 as

$$A(\mathbf{x}, z) = I_0 \frac{w_0}{w(z)} e^{-\frac{\|\mathbf{x}\|^2}{w(z)^2}} e^{-\frac{ik\|\mathbf{x}\|^2}{2R(z)}} e^{i \arg\left(\frac{1}{q(z)}\right)}, \quad (3.3)$$

where $\arg\left(\frac{1}{q(z)}\right)$ denotes the argument of the complex number $\frac{1}{q(z)}$. In particular, we obtain for the $z = 0$ -plane that

$$I(\mathbf{x}, z = 0) = I_0^2 e^{-2\frac{\|\mathbf{x}\|^2}{w_0^2}} \quad \text{and} \quad \phi(\mathbf{x}, z = 0) = \arg\left(\frac{1}{iz_R}\right), \quad (3.4)$$

which shows that the phase is constant, while the intensity is not. In our experimental setup we choose $I_0 = 1$, $k = 1$ and $z_R = 1$, such that $w_0 = \sqrt{\frac{2z_R}{k}} = \sqrt{2}$, which implies that

$$I(\mathbf{x}, z = 0) = e^{-\|\mathbf{x}\|^2} \quad \text{and} \quad \phi(\mathbf{x}, z = 0) = \arg\left(\frac{1}{i}\right) = \frac{3\pi}{2}. \quad (3.5)$$

For homogeneous Dirichlet-boundary conditions we again obtain the zero solution.

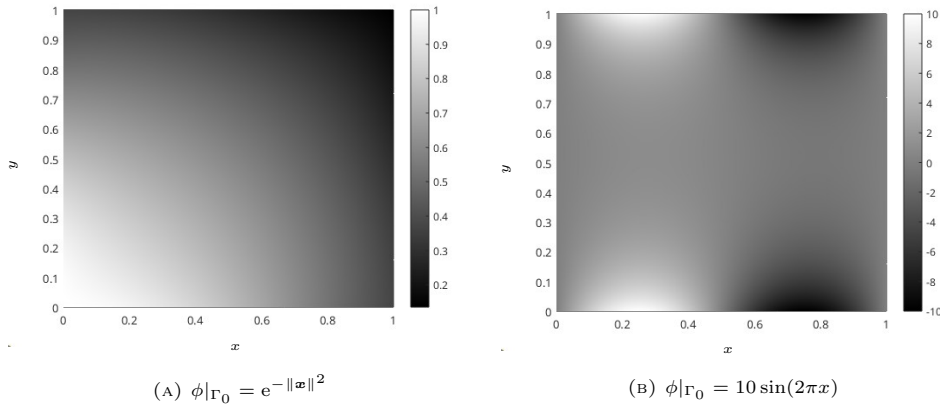


FIGURE 4. Reconstruction of the phase $\phi(\mathbf{x}, z = 0)$ described in Equation 3.5 with boundary data not corresponding to the ground-truth boundary value.

Figure 4 shows the solutions in the case that we impose boundary conditions that do not correspond to the known ground-truth boundary data. The results for the boundary value $e^{-\|\mathbf{x}\|^2}$ and $10 \sin(2\pi x)$ are depicted in Figure 4a and Figure 4b respectively. Again, we compute the phase given the ground-truth boundary data: The result is depicted in Figure 5a and we see that the phase is reconstructed reasonably well. Additionally, also plotting the error (see figure Figure 5b) confirms this.

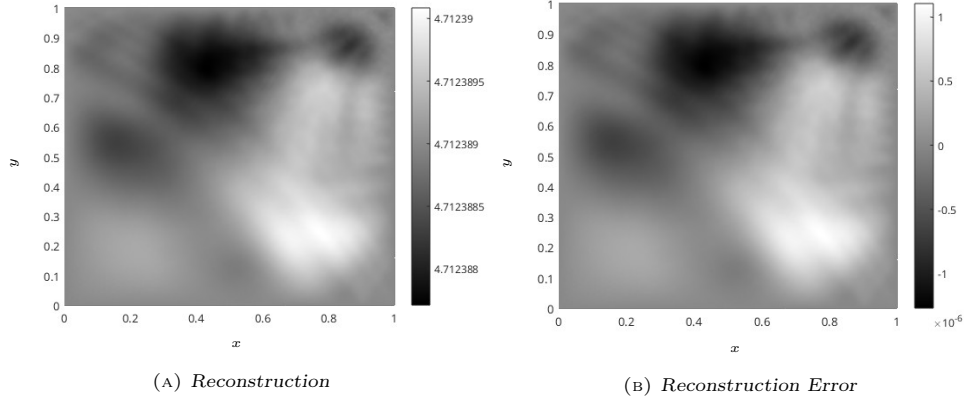


FIGURE 5. Reconstruction (left) and reconstruction error (right) of the phase $\phi(\mathbf{x}, z = 0)$ described in Equation 3.5 given the ground-truth boundary condition

4. SOLVING THE TRANSPORT OF PHASE EQUATION

In this section, we investigate methods for solving the nonlinear *transport of phase equation* Equation 1.4 with the method of characteristics and the viscosity method. With the first one we can obtain analytical solutions for special cases. The viscosity solutions provide approximate solutions, which can be calculated with finite element methods.

4.1. Characteristic method. The TIE allows us to compute the phase ϕ in Ω_0 and Ω_z with z close to 0 from phase data on Γ_0 and Γ_z (see Section 3.1). This however implies that phase measurements on 8 line segments (see Figure 1) need to be available. $\phi_z(\mathbf{x}, 0)$ is approximated by a difference quotient of ϕ in Ω_0 and Ω_z . So we consider Case 2 in Figure 1 and we investigate now the method of characteristics to determine local solutions in some examples analytically. We aim at finding a solution of Equation 1.4 on a curve starting from $(\mathbf{x}, 0) \in \Omega_0$ from given data

$$\phi(\mathbf{x}, 0) = g(\mathbf{x}, 0), \phi_z(\mathbf{x}, 0) = r(\mathbf{x}). \quad (4.1)$$

The TPE is a nonlinear partial differential equation of first order for a function $\phi : \mathbb{R}^3 \rightarrow \mathbb{R}$. We first formulate it as an algebraic equation

$$F(p, q, r, s, x, y, z) = 0, \quad (4.2)$$

where

$$F : \mathbb{R}^7 \rightarrow \mathbb{R},$$

$$(p, q, r, s, x, y, z) \mapsto 2kr - (p^2 + q^2) + \hat{I}(x, y, z)$$

and where the variables p, q, r, s satisfy

$$p = \phi_x, q = \phi_y, r = \phi_z, s = \phi.$$

Then we consider all variables parametrized with respect to $\tau \geq 0$, i.e.,

$$\begin{aligned} \tau &\mapsto x(\tau), \\ \tau &\mapsto y(\tau), \\ \tau &\mapsto z(\tau), \\ \tau &\mapsto s(\tau) = \phi(x(\tau), y(\tau), z(\tau)) \\ \tau &\mapsto p(\tau) = \phi_x(x(\tau), y(\tau), z(\tau)), \\ \tau &\mapsto q(\tau) = \phi_y(x(\tau), y(\tau), z(\tau)), \\ \tau &\mapsto r(\tau) = \phi_z(x(\tau), y(\tau), z(\tau)). \end{aligned}$$

After parametrization, the partial differential equation can be solved by computing the solution of the following ‘‘characteristic ODEs’’² (see [6, p 98]) with respect to τ :

$$\begin{aligned}
p' &= -\partial_x F - p\partial_s F = -\hat{I}_x \\
&= -\frac{(I_x^2 + I_y^2)I_x}{2I^3} + \frac{I_{xx}I_x + I_{yx}I_y}{2I^2} + \frac{I_x(I_{xx} + I_{yy})}{2I^2} - \frac{I_{xx}x + I_{yy}y}{2I}, \\
q' &= -\partial_y F - q\partial_s F = -\hat{I}_y \\
&= -\frac{(I_x^2 + I_y^2)I_y}{2I^3} + \frac{I_{xy}I_x + I_{yy}I_y}{2I^2} + \frac{I_y(I_{xx} + I_{yy})}{2I^2} - \frac{I_{xxy} + I_{yyy}}{2I}, \\
r' &= -\partial_z F - r\partial_s F = -\hat{I}_z \\
&= -\frac{I_z(I_x^2 + I_y^2)}{2I^3} + \frac{I_xI_{xz} + I_yI_{yz}}{2I^2} + \frac{I_z(I_{xx} + I_{yy})}{2I^2} - \frac{I_{xxz} + I_{yyz}}{2I}, \\
s' &= px' + qy' + rz', \\
x' &= \partial_p F = -2p, \quad y' = \partial_q F = -2q, \quad z' = \partial_r F = 2k.
\end{aligned} \tag{4.3}$$

On the characteristic curves, the rates of changes of x and y are determined by p and q , respectively. The derivative of z with respect to τ depends on the wave number k , while the derivatives of p , q , and r depend on the intensity I .

Example 4.1 I is uniform in xy -plane: $I(x, y, z) = \nu(z)$. From Equation 4.3 it follows that

$$\begin{aligned}
x' &= -2p, \quad y' = -2q, \quad z' = 2k, \\
s' &= px' + qy' + rz', \\
p' &= 0, \quad q' = 0, \quad r' = 0,
\end{aligned}$$

with the initial conditions

$$F(x_0, y_0, z_0, s_0, p_0, q_0, r_0) = 2kr_0 - (p_0^2 + q_0^2) + \hat{I}(x_0, y_0, z_0) = 0$$

and

$$\begin{aligned}
x(0) &= x_0, \quad y(0) = y_0, \quad z(0) = z_0, \\
s(0) &= g(x_0, y_0, z_0), \\
p(0) &= p_0, \quad q(0) = q_0, \quad r(0) = r_0.
\end{aligned}$$

Thus the solutions of the characteristic equations are given by

$$\begin{aligned}
x(\tau) &= -2p_0\tau + x_0, \quad y(\tau) = -2q_0\tau + y_0, \quad z(\tau) = 2k\tau + z_0, \\
s(\tau) &= (-2p_0^2 - 2q_0^2 + 2kr_0)\tau + s_0 \\
p(\tau) &= p_0, \quad q(\tau) = q_0, \quad r(\tau) = r_0.
\end{aligned} \tag{4.4}$$

Based on the $x(\tau)$, $y(\tau)$, $z(\tau)$, $s(\tau)$, $p(\tau)$, $q(\tau)$ and $r(\tau)$ above, we can derive the solution of Equation 4.1 in explicit form

$$\phi = p_0(x - x_0) + q_0(y - y_0) + r_0z + g(x_0, y_0, z_0).$$

In other words, if we know the phase and its derivative at a point (x_0, y_0, z_0) , we know it along the line specified in Equation 4.4.

Example 4.2 (Gaussian beam) The intensity of the Gaussian beam, as defined in Equation 3.3, is given by

$$I(\mathbf{x}, z) = I_0 \frac{w_0^2}{w^2(z)} e^{-2\frac{\|\mathbf{x}\|^2}{w^2(z)}} \text{ with } I_0 > 0 \text{ and } w(z) = w_0 \sqrt{1 + \frac{z^2}{z_R^2}},$$

and we take initial conditions as $p(0) = p_0$, $q(0) = q_0$, $r(0) = r_0$, $\phi(0) = 0$. The ODE system Equation 4.3 then becomes

$$\begin{aligned}
x' &= -2p, \quad y' = -2q, \quad z' = 2k, \\
s' &= px' + qy' + rz', \\
p' &= -8xw^{-4}, \quad q' = -8yw^{-4}, \quad r' = -((8zz_R^2(-2(x^2 + y^2)z_R^2 + w_0^2(z^2 + z_R^2)))/(w_0^4(z^2 + z_R^2)^3)).
\end{aligned}$$

However, it is difficult to solve this ODE system. In the following we use the viscosity method to find an approximate solution of the TPE.

^{2.} denotes the derivative with respect to τ .

4.2. Viscosity Solutions of the TPE. Let $\epsilon > 0$. The viscosity approximation of the TPE, Equation 1.4, is given by:

$$\begin{cases} \phi_z^\epsilon(\mathbf{x}, z) - \frac{\epsilon \Delta_{\mathbf{x}} \phi^\epsilon(\mathbf{x}, z)}{2k} - \frac{\|\nabla_{\mathbf{x}} \phi^\epsilon(\mathbf{x}, z)\|^2}{2k} = -\frac{1}{2k} \hat{I}(\mathbf{x}, z), & (\mathbf{x}, z) \in \Omega \\ \phi^\epsilon(\mathbf{x}, 0) = g(\mathbf{x}), & (\mathbf{x}, 0) \in \Omega_0. \end{cases} \quad (4.5)$$

Recall that $\Omega = [0, 1]^3$ and $\Omega_0 = [0, 1]^2 \times \{z = 0\}$ and g is the initial value (at $z = 0$). If the limit ϕ^ϵ , $\epsilon \rightarrow 0+$ exists, then it is considered a generalized solution of the TPE and it is named the *vanishing viscosity solution* [3]. Therefore, the fully nonlinear TPE is approximated by a quasilinear parabolic partial differential equation Equation 4.5. The additional term $\epsilon \Delta \phi^\epsilon$ acts as a regularizer.

4.2.1 Solution of the quasilinear PDE

We use the Cole-Hopf transformation (see [6, p 206]) to transform Equation 4.5 to a linear equation, which can be solved with standard numerical methods. The Cole-Hopf transformation ψ^ϵ of ϕ^ϵ , which is defined through the relation

$$\phi^\epsilon(\mathbf{x}, z) = \epsilon \log \psi^\epsilon(\mathbf{x}, z), \quad (\mathbf{x}, z) \in \Omega$$

satisfies

$$\begin{cases} \psi_z^\epsilon(\mathbf{x}, z) - \frac{\epsilon \Delta_{\mathbf{x}} \psi^\epsilon(\mathbf{x}, z)}{2k} + \frac{\hat{I}(\mathbf{x}, z)}{2k\epsilon} \psi^\epsilon(\mathbf{x}, z) = 0, & (\mathbf{x}, z) \in \Omega \\ \psi^\epsilon(\mathbf{x}, 0) = \exp\left(\frac{g(\mathbf{x})}{\epsilon}\right), & (\mathbf{x}, 0) \in \Omega_0 \\ \psi^\epsilon(\mathbf{x}, z) = \exp\left(\frac{3\pi}{2\epsilon}\right), & (\mathbf{x}, z) \in \partial\Omega. \end{cases} \quad (4.6)$$

Here we have used that

$$\phi_z^\epsilon(\mathbf{x}, z) = \frac{\epsilon}{\psi^\epsilon(\mathbf{x}, z)} \psi_z^\epsilon(\mathbf{x}, z), \quad \Delta_{\mathbf{x}} \phi^\epsilon(\mathbf{x}, z) = \frac{\epsilon \Delta_{\mathbf{x}} \psi^\epsilon(\mathbf{x}, z)}{\psi^\epsilon(\mathbf{x}, z)} - \frac{\epsilon \|\nabla_{\mathbf{x}} \psi^\epsilon(\mathbf{x}, z)\|^2}{\psi^\epsilon(\mathbf{x}, z)^2}, \quad \nabla_{\mathbf{x}} \phi^\epsilon(\mathbf{x}, z) = \frac{\epsilon \nabla_{\mathbf{x}} \psi^\epsilon(\mathbf{x}, z)}{\psi^\epsilon(\mathbf{x}, z)}.$$

We study similar examples as we studied for the TIE equation:

Example 4.3 We assume a Gaussian beam intensity $I(\mathbf{x}, z) = I_0 \frac{w_0}{w(z)} \exp\left(-2 \frac{\|\mathbf{x}\|^2}{w(z)^2}\right)$ as in Equation 3.3. ϕ^ϵ is solved along the z -axis by solving first Equation 4.6 for ψ^ϵ and Cole-Hopf transformation later.

With Dirichlet boundary conditions $\psi^\epsilon = \exp\left(\frac{3\pi}{2\epsilon}\right)$ Equation 4.6 is uniquely solvable in the domain $[0, 1]^3$. The viscosity parameter ϵ was chosen as $5e - 2$. In our numerical setting, z values correspond to the wave propagating along the z axis from 0 to 1. The true phase is given in Equation 3.3. After transforming back to ϕ^ϵ , the numerical solution and error at $z = 0.1, 0.5, 1$ of the Equation 4.5 are shown in Figure 6 and Figure 7:

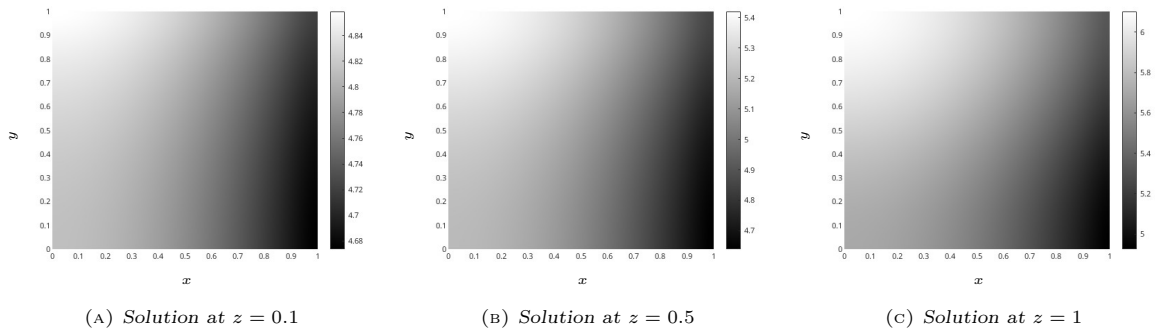


FIGURE 6. Snapshots of viscosity solutions for ϕ when $z = 0.1, 0.5, 1$ in Example 4.3. Given the result of the TIE in Figure 5a we used them as initial condition for the TPE. The results show the solution of the TPE in z -directions.

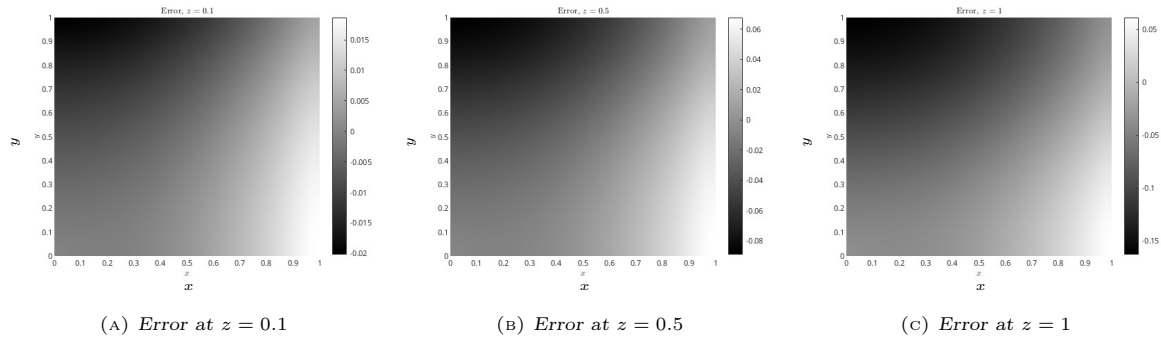


FIGURE 7. Snapshots of relative viscosity solution errors for ϕ when $z = 0.1, 0.5, 1$ in Example 4.3, which increases approximately from 5% to about 15%.

5. CONCLUSION

In this paper, we derived the TIE and the TPE from the paraxial Helmholtz equation (see Equation 2.8). We considered two solutions of Equation 2.8 for testing the performance of the reconstructions. The first example presented in Section 3.1 had constant intensity, as a second example we considered the Gaussian beam (see Section 3.2). We have reconstructed the phase given intensity measurements in the $z = 0$ -plane by solving the TIE in Section 3. For this we had to impose boundary conditions on Γ_0 and reconstructed the phase on the two-dimensional domain Ω_0 as depicted in Case 1 of Figure 1. It was shown that with ground-truth boundary conditions the reconstruction with the TIE works reasonably well, while imposing an arbitrary boundary condition resulted in significant deviations from the ground-truth. We showed the corresponding numerical results in Figure 2, Figure 3, Figure 4 and Figure 5.

In Section 4 we considered hybrid reconstruction of the phase in the 3-dimensional domain Ω following the strategy of Case 2 of Figure 1. Our current results are limited to the viscosity setting and the method of characteristic can be only used in exceptional cases.

Acknowledgements. This research was funded in whole, or in part, by the Austrian Science Fund (FWF) 10.55776/P34981 – New Inverse Problems of Super-Resolved Microscopy (NIPSUM) and SFB 10.55776/F68 “Tomography Across the Scales”, project F6807-N36 (Tomography with Uncertainties). For the purpose of open access, the author has applied a CC BY public copyright license to any Author Accepted Manuscript version arising from this submission. The financial support by the Austrian Federal Ministry for Digital and Economic Affairs, the National Foundation for Research, Technology and Development and the Christian Doppler Research Association is gratefully acknowledged.

REFERENCES

- [1] R. A. Adams and J. J. F. Fournier. “Sobolev Spaces: Volume 140”. en. 2nd ed. Pure and Applied Mathematics (Amsterdam). San Diego, CA: Academic Press, June 2003 (cited on page 5).
- [2] E. Bostan, E. Froustey, M. Nilchian, D. Sage, and M. Unser. “Variational Phase Imaging Using the Transport-of-Intensity Equation”. In: *IEEE Transactions on Image Processing* 25.2 (2016), pp. 807–817. ISSN: 1057-7149. DOI: [10.1109/tip.2015.2509249](https://doi.org/10.1109/tip.2015.2509249) (cited on pages 1, 2, 5).
- [3] M. G. Crandall and P.-L. Lions. “Viscosity solutions of Hamilton-Jacobi equations”. In: *Transactions of the American Mathematical Society* 277.1 (1983), pp. 1–42. DOI: [10.1090/s0002-9947-1983-0690039-8](https://doi.org/10.1090/s0002-9947-1983-0690039-8) (cited on pages 3, 10).
- [4] C. David, B. Nöhammer, H. H. Solak, and E. Ziegler. “Differential x-ray phase contrast imaging using a shearing interferometer”. In: *Applied Physics Letters* 81.17 (2002), pp. 3287–3289. DOI: [10.1063/1.1516611](https://doi.org/10.1063/1.1516611) (cited on page 1).
- [5] H. W. Engl. “Integralgleichungen”. Vienna: Springer Verlag, 1997 (cited on page 2).
- [6] L. Evans. “Partial Differential Equations”. 2010. DOI: [10.1090/gsm/019](https://doi.org/10.1090/gsm/019) (cited on pages 5, 9, 10).
- [7] J. R. Fienup. “Reconstruction of an object from the modulus of its Fourier transform”. In: *Optics Letters* 3.1 (1978), p. 27. DOI: [10.1364/ol.3.000027](https://doi.org/10.1364/ol.3.000027) (cited on page 1).

-
- [8] R. Fitzgerald. “Phase-Sensitive X-Ray Imaging”. In: *Physics Today* 53.7 (2000), pp. 23–26. DOI: [10.1063/1.1292471](https://doi.org/10.1063/1.1292471) (cited on page 1).
- [9] H. D. Geissinger and C. L. Duitschaever. “Nomarski differential-interference contrast microscopy in transillumination: Its use on unstained or stained sections, smears, and wet mounts, or on fluorochromed sections and cell-culture monolayers”. In: *Journal of Microscopy* 94.2 (1971), pp. 107–124. ISSN: 1365-2818. DOI: [10.1111/j.1365-2818.1971.tb03695.x](https://doi.org/10.1111/j.1365-2818.1971.tb03695.x) (cited on page 1).
- [10] R. Gerchberg and W. Saxton. “A practical algorithm for the determination of the phase from image and diffraction plane pictures”. In: *Optik* 35.2 (1972), pp. 237–246. ISSN: 0030-4026 (cited on page 1).
- [11] J. W. Goodman. “Introduction to Fourier Optics”. en. 2nd ed. McGraw-Hill series in electrical and computer engineering. Electromagnetics. London, England: McGraw-Hill Publishing, Mar. 1996 (cited on page 3).
- [12] T. E. Gureyev, A. Roberts, and K. A. Nugent. “Phase retrieval with the transport-of-intensity equation: matrix solution with use of Zernike polynomials”. In: *Journal of the Optical Society of America A* 12.9 (1995), p. 1932. ISSN: 0764-583X. DOI: [10.1364/josaa.12.001932](https://doi.org/10.1364/josaa.12.001932) (cited on pages 2, 3).
- [13] W. Hackbusch. “Elliptic Differential Equations”. 2017. DOI: [10.1007/978-3-662-54961-2](https://doi.org/10.1007/978-3-662-54961-2) (cited on page 5).
- [14] J. Petrucci, L. Tian, and G. Barbastathis. “The transport of intensity equation and partially coherent fields”. In: *Biomedical Optics, BIOMED 2012* (Apr. 2012). DOI: [10.1364/BIOMED.2012.BSu3A.69](https://doi.org/10.1364/BIOMED.2012.BSu3A.69) (cited on pages 2, 5).
- [15] F. Roddier. “Wavefront sensing and the irradiance transport equation”. In: *Applied Optics* 29.10 (1990), p. 1402. DOI: [10.1364/ao.29.001402](https://doi.org/10.1364/ao.29.001402) (cited on page 2).
- [16] B. E. A. Saleh and M. C. Teich. “Fundamentals of Photonics, 2 Volume Set”. 3rd ed. Wiley Series in Pure and Applied Optics. Nashville, TN: John Wiley & Sons, Mar. 2019 (cited on pages 3, 4, 6).
- [17] C. U. Strohmenger. *Phase retrieval using the transport of intensity equation*. eng. Wien, 2023 (cited on page 5).
- [18] M. R. Teague. “Deterministic phase retrieval: a Green’s function solution”. In: *Journal of the Optical Society of America* 73.11 (1983), p. 1434. DOI: [10.1364/josa.73.001434](https://doi.org/10.1364/josa.73.001434) (cited on pages 1, 2).
- [19] C. Zuo, J. Li, J. Sun, Y. Fan, J. Zhang, L. Lu, R. Zhang, B. Wang, L. Huang, and Q. Chen. “Transport of intensity equation: a tutorial”. In: *Optics and Lasers in Engineering* 135 (Dec. 2020), p. 106187. DOI: [10.1016/j.optlaseng.2020.106187](https://doi.org/10.1016/j.optlaseng.2020.106187) (cited on page 1).